U.S. DEPARTMENT OF ENERGY | Office of Science

NSTX-U

Vacuum ultraviolet and Ultraviolet Spectrometers for Real-time Radiative Divertor Feedback Control in the NSTX-U Tokamak

V. A. Soukhanovskii, R. Kaita, B. Stratton, and NSTX-U Team

Lawrence Livermore National Laboratory

PPPL

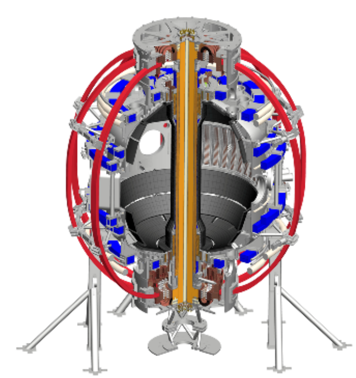

Abstract

To prevent excessive erosion and thermal damage of divertor plasma-facing components, a radiative divertor technique is planned for the NSTX-U tokamak. In the radiative (partially detached) divertor, plasma volumetric power and momentum losses are significantly increased by means of extrinsically seeded deuterium or impurity gases. A real-time feedback control of the gas seeding rate (the actuator) is planned. The control sensors can include a variety of diagnostics; however, to make the radiative divertor control independent of main plasma discharge parameters (e.g., input power, plasma current, density, seeding gas, etc), we consider divertor plasma electron temperature as a control parameter. During divertor detachment, a radiation front is formed at 10-15 eV if low-Z impurities (e.g., carbon, nitrogen) are used for radiation. In the strike point region, strong deuterium high-*n* Balmer and Paschen series line emissions are observed. A vacuum ultraviolet spectrometer SPRED with a fast camera detector is developed for temperature monitoring at T_e < 15 eV, based on the *Dn*=0,1,2 line intensity ratios of low-Z lines in the spectral range 300-1600 A. A separate multichannel ultraviolet spectrometer is used for temperature measurements based on the Balmer line intensities at T_e < 5 eV. Both spectrometers use collisional-radiative model based line intensity ratio interpretation and output a real-time T_e-dependent signal within a characteristic divertor detachment equilibration time of ≤ 15 ms.

Prepared under Contracts DE-AC52-07NA27344 and DE-AC02-09CH11466.

Outline

- Radiative divertor technique in standard and snowflake configurations are leading heat flux mitigation candidates in NSTX-U
- Real-time T_e from two spectrometers is proposed as control signal for radiative divertor control
  - VUV spectrometer SPRED – carbon and nitrogen ion emission lines for 5 eV ≤ T_e ≤ 25 eV
  - UV spectrometer DIBS – deuterium Balmer lines and recombination continuum for T_e ≤ 0.5-3 eV

Various techniques developed for reduction of heat fluxes $q_{||}$ (divertor SOL) and q_{peak} (divertor target)

Radiated power loss Increase via V_{div}, $L_{||}$

Poloidal target inclination, up-down, in-out fractions, N divertors

$$q_{peak} \simeq \frac{P_{div}}{A_{wet}} = \frac{P_{SOL}(1 - f_{rad}) f_{geo}}{2\,\pi R_{SP} f_{exp} \lambda_{q_{||}}}$$

Increase plasma-wetted area

Increase divertor area at large R_{SP}

Increase plasma-wetted area via increasing f_{exp}

Increase λ_q via increased radial transport, $L_{||}$

Divertor peak heat flux mitigation techniques:

- Divertor geometry (poloidal flux expansion, divertor plate tilt, magnetic balance, snowflake divertor)
  - Radiative divertor with extrinsic impurity seeding

Open geometry divertor with graphite PFCs will be used in initial years in NSTX Upgrade

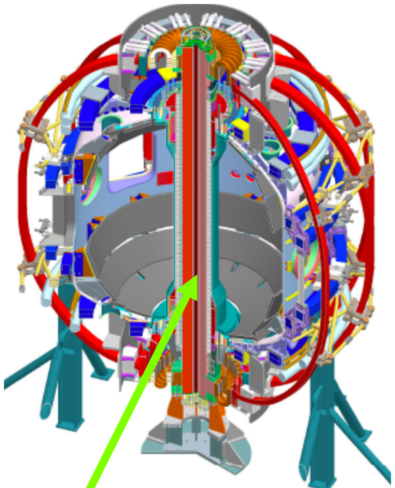

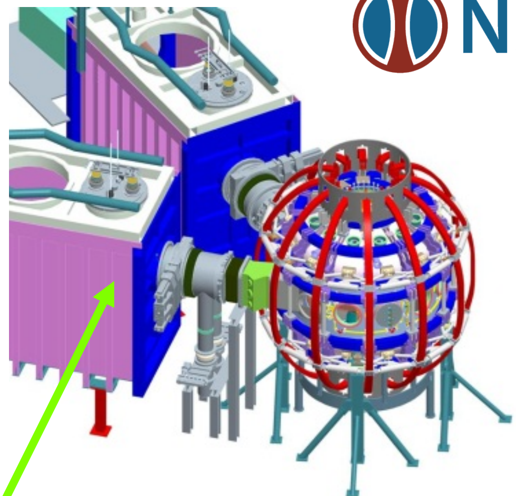

New center-stack **2^{nd} neutral beam**

B_T	→ 1 T	P_{NBI}	→ 12 MW
I_p	→ 2 MA	pulse	→ 5 s

J. E. Menard et. al, Nucl. Fusion 52 (2012) 083015

- Open divertor geometry
- No active divertor pumping
- Graphite plasma facing components
- Four up-down symmetric divertor coils
- Diagnostics: IR cameras, MPTS, Langmuir probes, filtered visible cameras, VUV-UV-VIS-NIR spectroscopy

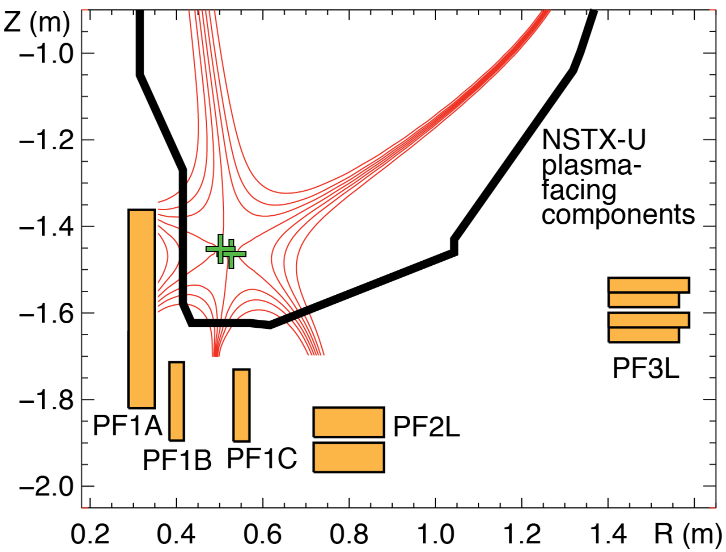

Edge modeling predicts significant heat flux reduction with radiative snowflake divertor

- Snowflake with 3% carbon
- Wide density operational window as low as $n_e/n_G \leq 0.4$
  - Peak heat flux reduced up to 50% stronger (cf. standard radiative divertor) at lower n_e
  - Less impurity seeding (argon or neon) needed for lower peak heat flux
- Multi-fluid code UEDGE
  - B_t = 1.0 T, I_p = 2 MA, P_{SOL} = 9 MW
  - NSTX-like transport $\chi_{i,e}$=2-4 m^2/s, D=0.5 m^2/s

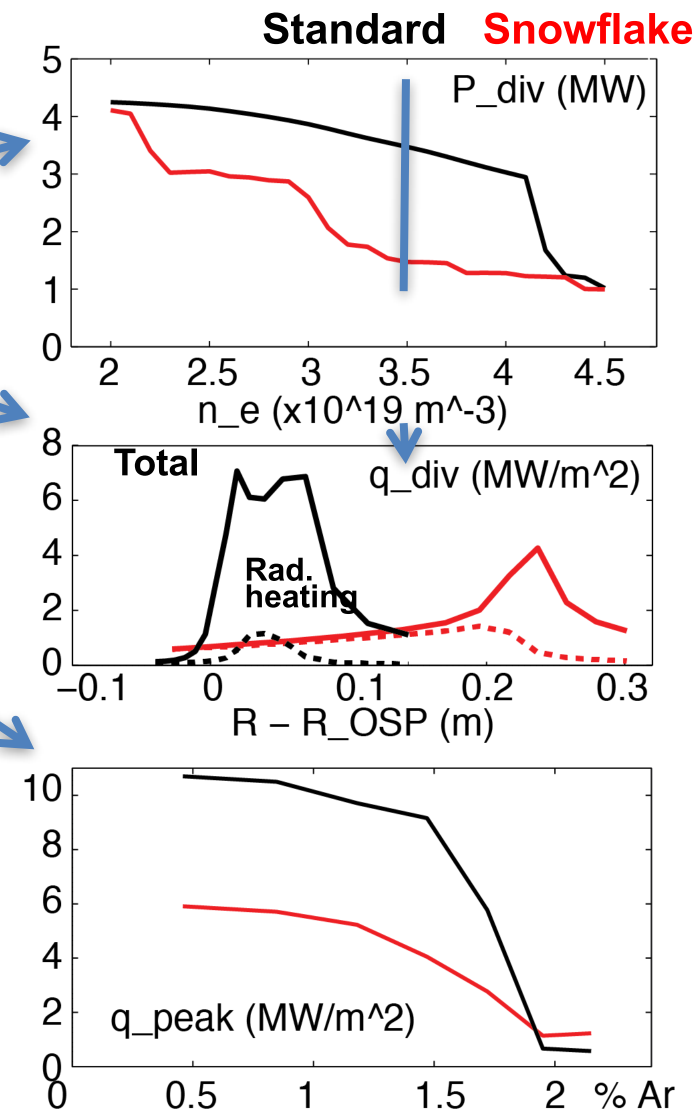

E. T. Meier et. al, Nucl. Fusion (2015)

Impurity-seeded radiative divertor with feedback control is planned for long discharges

- In NSTX, heat flux reduction in radiative divertor compatible with H-mode confinement was demonstrated with D_2 or CD_4 puffing
- Feedback control of divertor radiation via impurity particle balance control
  - Cryopump for particle removal
  - Divertor gas injectors
  - Real-time control signal diagnostics could include
    - PFC temperature via IR thermography or thermocouple
    - Thermoelectric current between inner and outer divertor
    - Impurity VUV spectroscopy or bolometry
    - Neutral gas pressure or electron-ion recombination rate
    - Spectroscopic T_e estimation

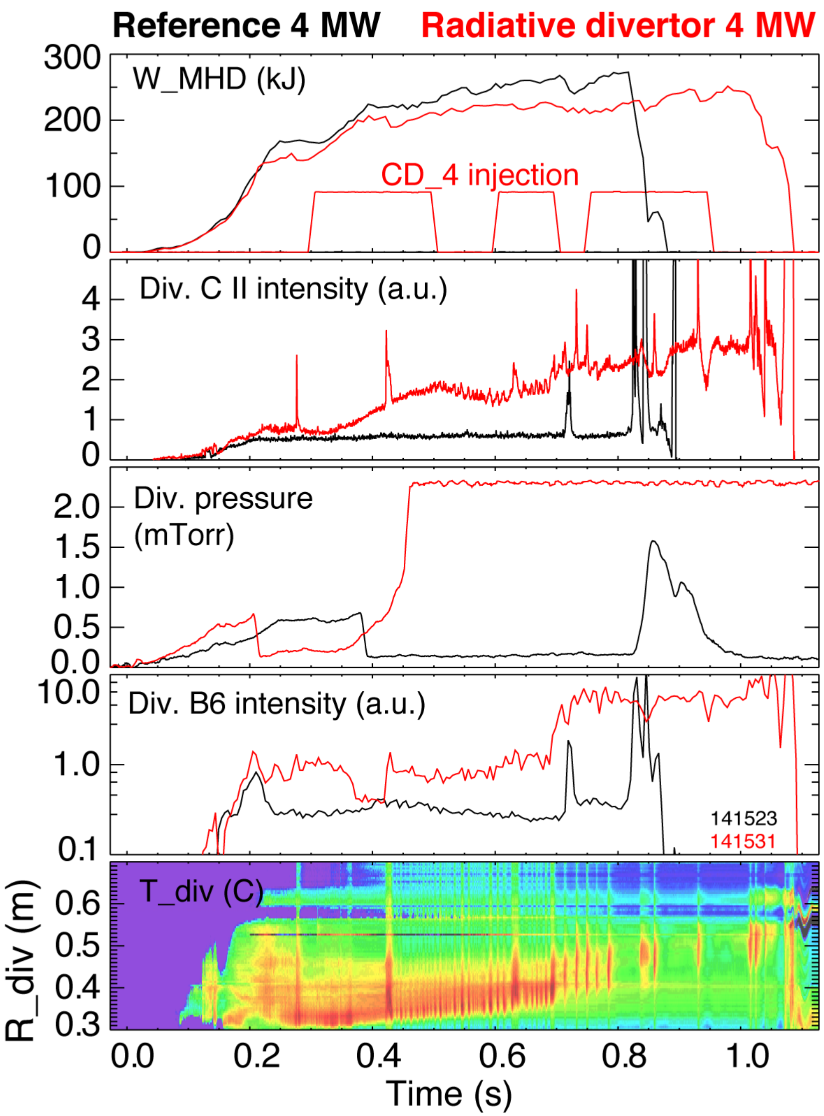

Soukhanovskii, HTPD 2012, RSI 2012

Conceptual design of radiative divertor feedback control system is based on PID control

- Proportional, integral, derivative controller

$$\Delta S = S_c - S_{ref}$$

$$V = K_0 + K_p \Delta S + K_i \int_{t_1}^{t_2} \Delta S dt + K_d \frac{d\Delta S}{dt}$$

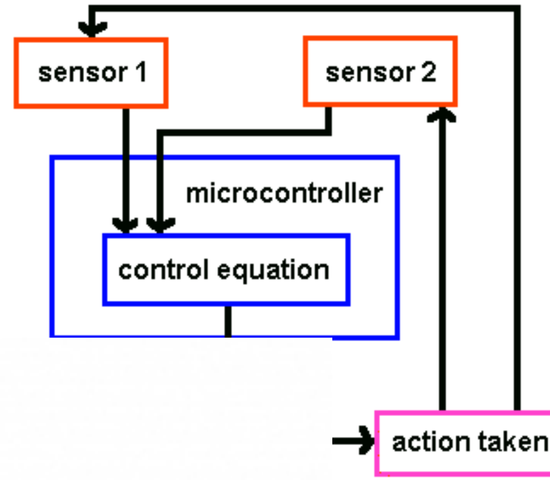

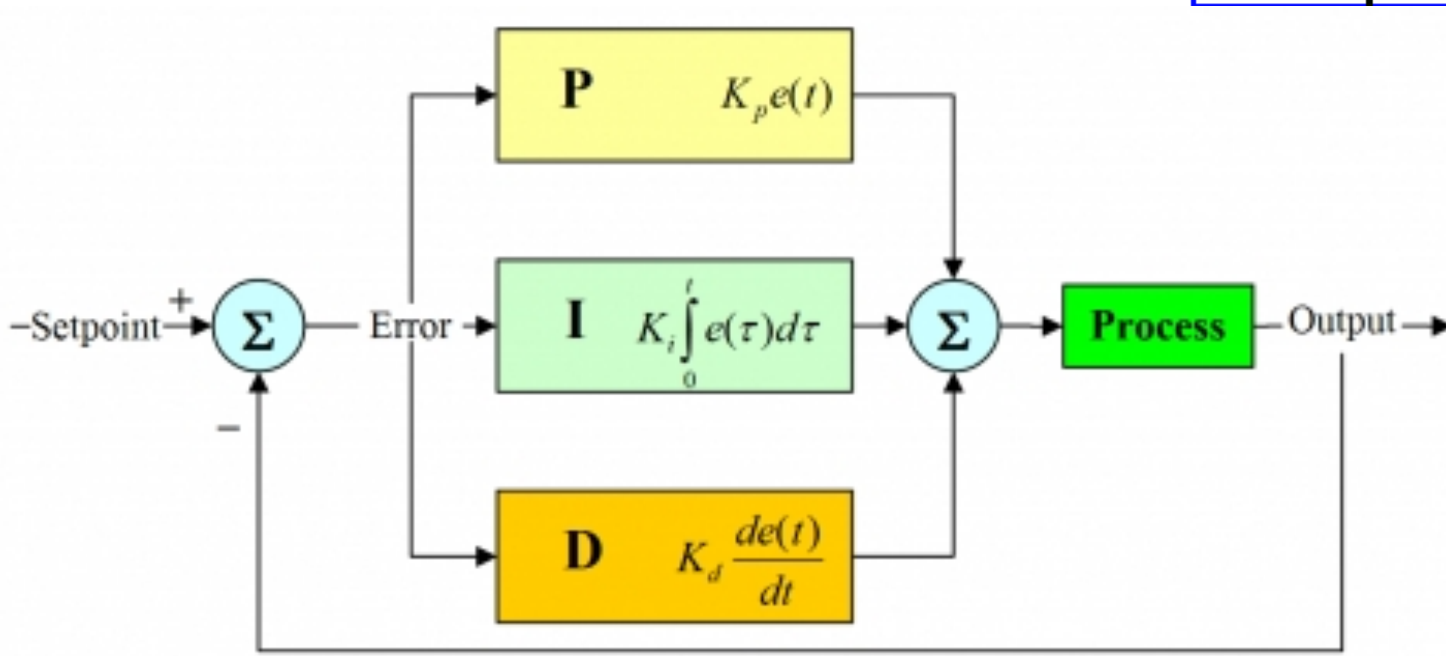

Control actuator – the new divertor gas injection system is being commissioned

- Four ½" OD SS divertor gas injection lines
- 2 upper and 2 lower
  - Copper backing plates modified to run tubing
  - Piezoelectric valves located at L=50 ms x v_c from orifice
  - $\Gamma \leq$ 1e22 particles/s

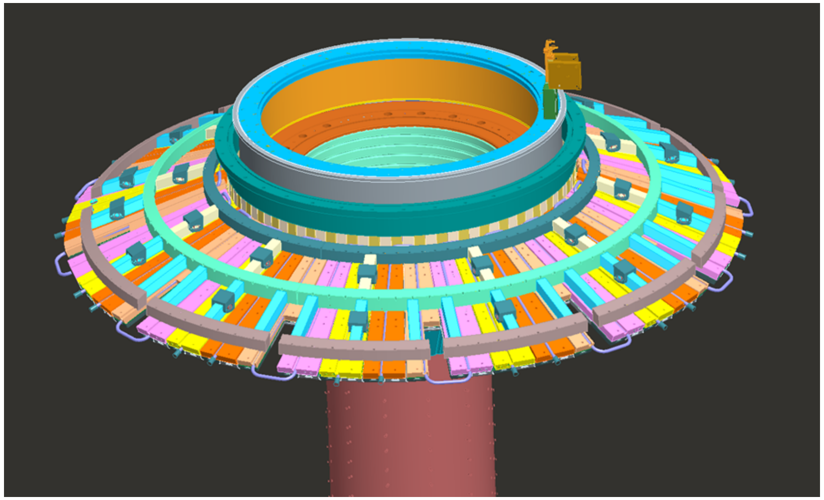

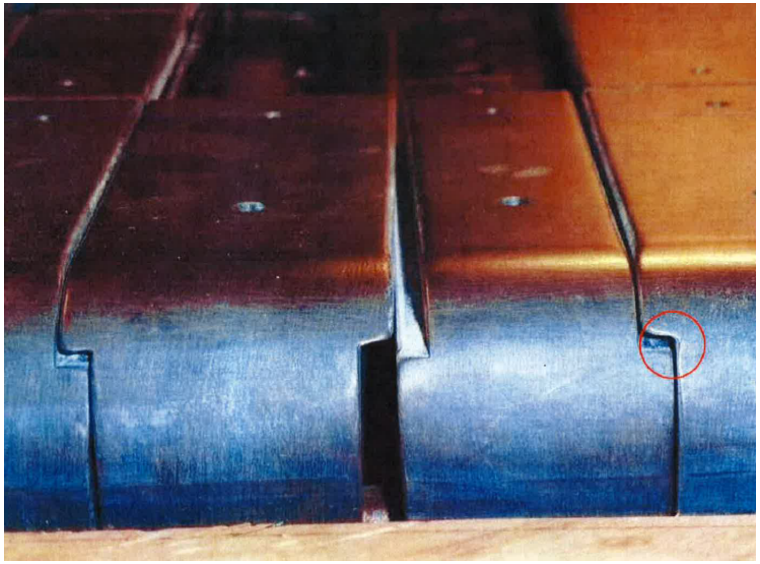

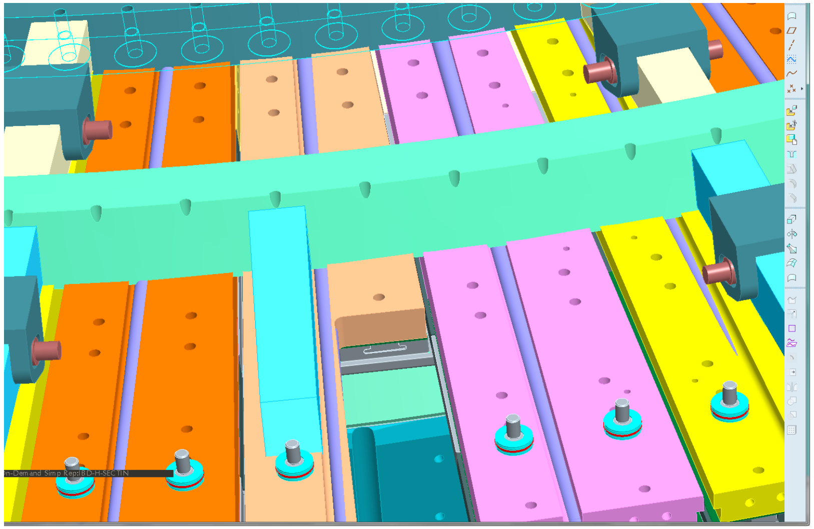

T_e-sensitive line intensity ratios are considered for divertor detachment control signal

- Balmer n=6-12 series lines in ion-neutral interaction zone $T_e \leq 5$ eV
  - Population kinetics is dominated by 3-body recombination at lower temperature
  - 3-body recombination rate

    $R \sim n_e^3\, T_e^{-4.5}$
  - Plasma is optically thin for Balmer lines
  - Dominated by Stark broadening due to linear Stark effect in electron and ion microfield. Other mechanisms neglected: Zeeman spitting, Van der Waals and natural broadening
  - Background due to bremsstrahlung and radiative recombination

$$\epsilon = 1.89 \times 10^{-28}\, \frac{n_e^2\, g_{ff}\, Z_{eff}}{\lambda^2 \sqrt{T_e}}\, e^{-\frac{12400}{T_e\, \lambda}}$$

$$I_{Z,z-1,n} = I_H \frac{z^2}{n^2} \qquad \frac{I_{Z,z-1,n}}{kT} \leq \frac{hc}{\lambda kT}$$

$$\frac{dP(\lambda,T)}{d\lambda} = \frac{2.051\times 10^{-19}\, g_{ff}(z,\lambda,T)}{\lambda^2\, \sqrt{T_e}}\, \frac{I_H}{kT} N_e\, e^{\frac{hc}{\lambda kT}} \sum_{Z,z,n} g_{fb} \frac{\eta_{Z,z,n}}{n} \left(\frac{I_{Z,z-1,n}}{kT}\right)^2 \frac{N(Z^{+z})}{N(Z)} \frac{N(Z)}{N(H)} N(H)\, e^{\frac{I_{Z,z-1,n}}{kT}}$$

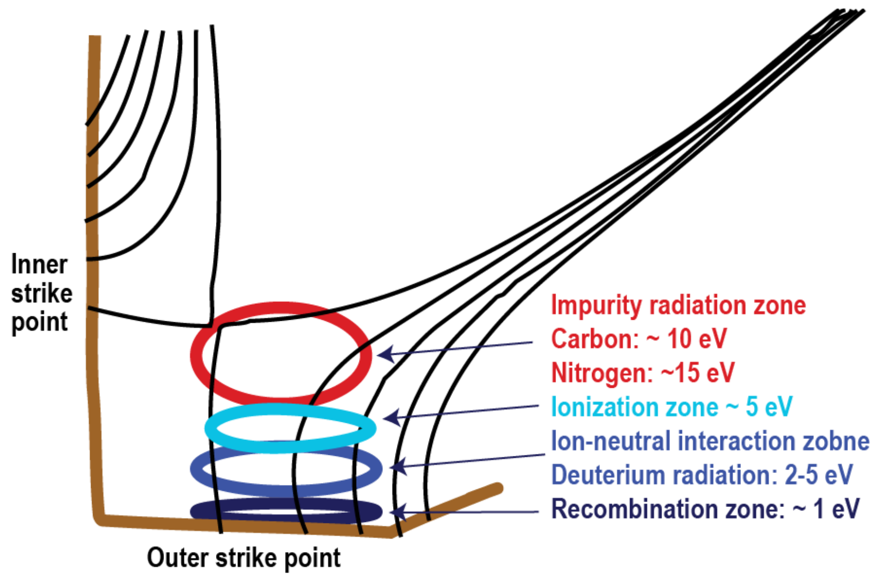

Figure concept after M. E. Fenstermacher, PPCF 1999

- Carbon or nitrogen Δn=0; 1; 2 lines in impurity radiation zone $T_e \leq 10$-15 eV
  - Intensity ratios highly T_e sensitive due to T_e sensitivity of excitation rates
  - Emission also proportional to impurity density

Carbon or nitrogen Li-like and Be-like ion Δn=0; 1; 2 line intensity ratios are T_e sensitive

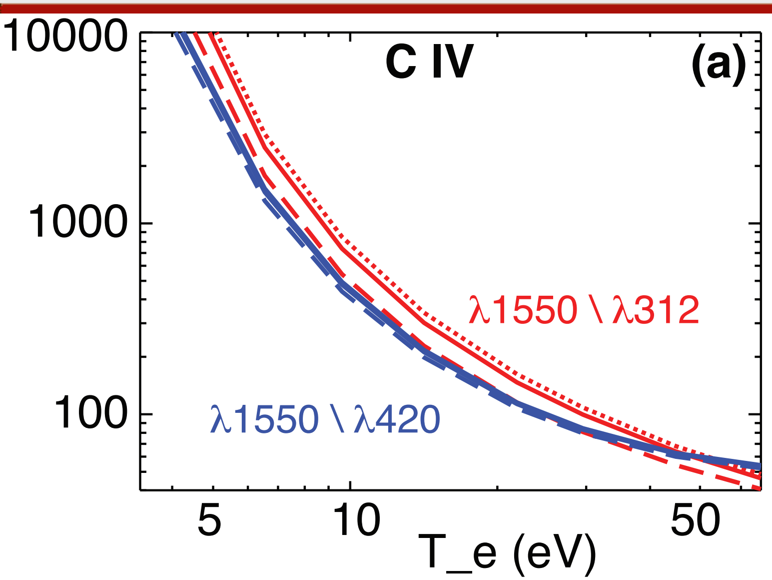

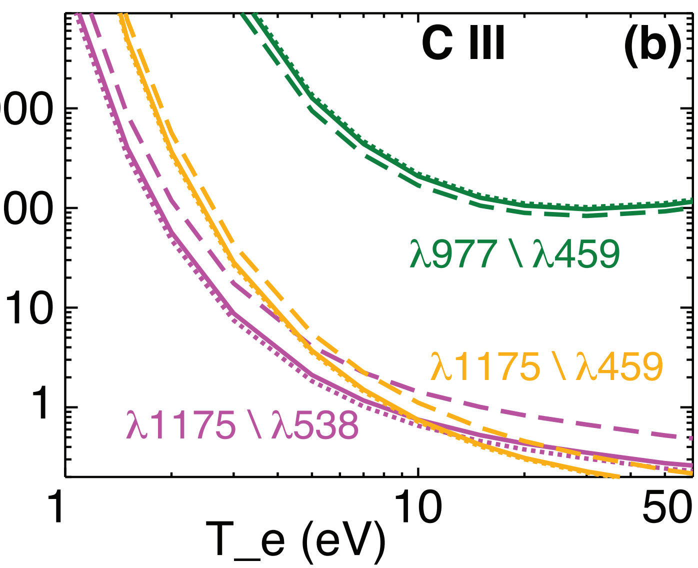

TABLE I. Select unblended carbon and nitrogen ion $\Delta n = 0$ and $\Delta n = 1$ emission lines that can form T_e-sensitive line intensity ratios.

Isosequence	Transition	Wavelength (Å) Carbon	Nitrogen
Li I	$2s\ ^2S_{1/2} - 2p\ ^2P_{3/2}$	1548.2	1238.8
	$2s\ ^2S_{1/2} - 2p\ ^2P_{1/2}$	1550.8	1242.8
	$2p\ ^2P - 3s\ ^2S$	419.6	266.3
	$2s\ ^2S - 3p\ ^2P$	312.4	209.3
Be I	$2s^2\ ^1S_0 - 2s2p\ ^1P_1$	977.0	765.2
	$2s2p\ ^3P - 2p^2\ ^3P$	1175.6	923.1
	$2s2p\ ^3P - 2s3s\ ^3S$	538.2	322.6
	$2s2p\ ^3P - 2s3d\ ^3D$	459.6	335.0

- Δn=0 and Δn=1 are baseline approach
- Δn=2 transitions can also be considered if reliably measured
- ADAS PECs used (PEC93)

← Lines correspond to three densities 2, 5, 20 x 10^{19} m^{-3}

Divertor SPRED spectrometer has broad applications for NSTX-U program

- Support plasma-facing component program
  - Steady-state and transient divertor impurity measurements
    - edge / divertor Mo III-XIV line emission
    - SOL / divertor Li II, Li III, C II, C III, C IV line emission
- Support divertor program
  - Divertor carbon ionization balance (steady-state and during ELMs)
  - Divertor T_e estimates from C II, C III, C IV line ratio (LR) measurements
    - Deviation from Maxwellian EEDF might be detected from these LR's
  - Improved divertor P_{rad} analysis
    - Most P_{rad} is due to several strong C III - C IV emission lines in the VUV
  - Radiative divertor impurity radiation (CD_4, N_2, Ne, Ar)
  - Detached divertor Lyman series for recombination rate, T_e, opacity

Divertor SPRED VUV spectrometer enables impurity emission measurement in outer divertor leg

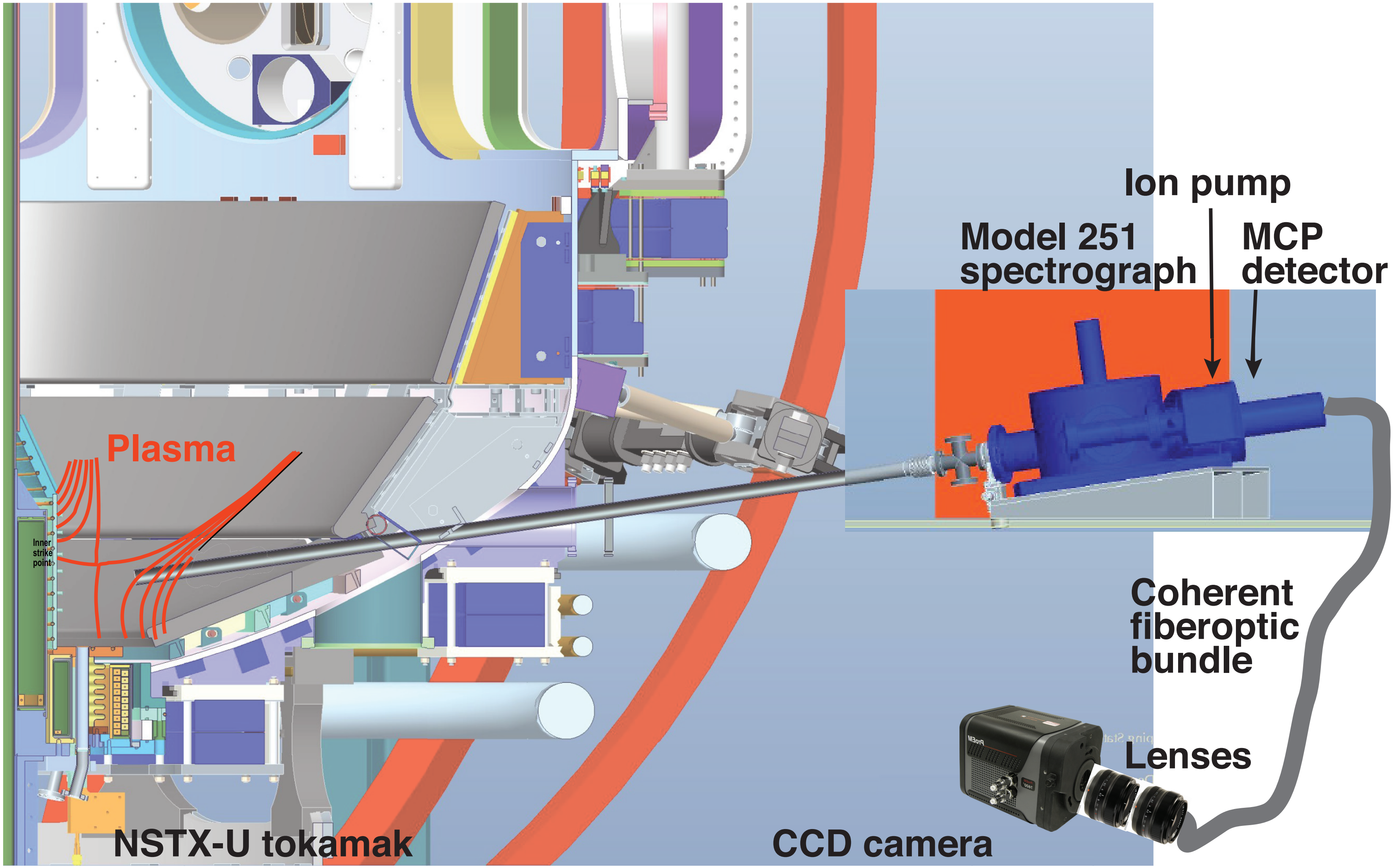

VUV spectrometer SPRED

- McPherson Model 251 flat-field 0.3 m spectrograph (Weight: 250 lb)
- Two-grating turret with Au-coated gratings 290 and 2105 l/mm
- MCP-based detector with CsI-coated photocathode and P46 phosphor
  - Time response 50 um
- Ion pump with controller
- Schott 12 ft imaging bundle 25x4 mm
- Princeton Instruments Pro-EM 1600x200 camera
  - Electron multiplication gain 1-1000
  - 16 um pixels
  - Readout time if fully vertically binned 0.70 ms
  - Readout time if single row 0.22 ms

Laboratory spectral measurements with divertor SPRED

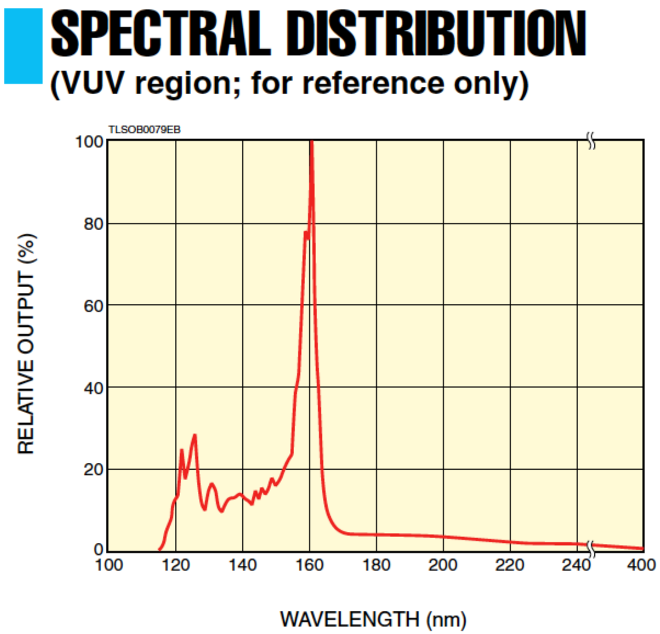

- Hamamatsu VUV D_2 lamp
- Laboratory SPRED measurements performed through a MgF_2 window – hence the cut-off at about 1150 A

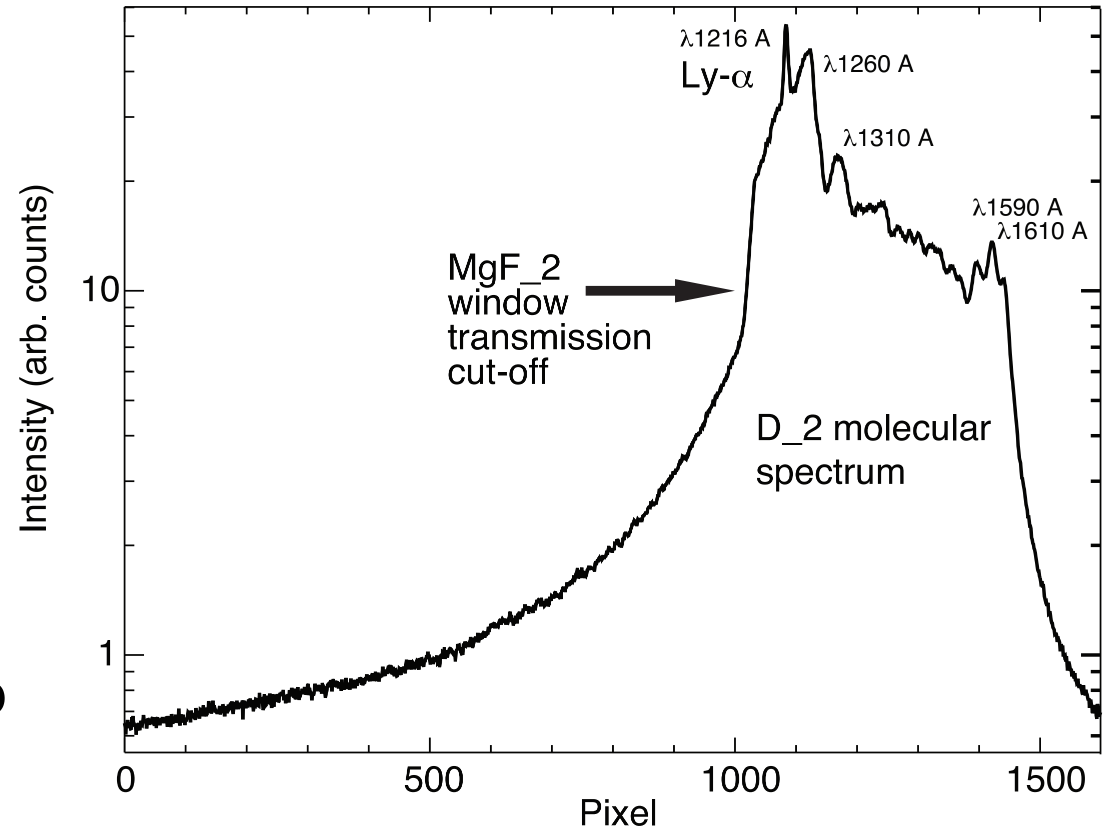

- Laboratory measurements show high dynamic range of the detector system
- Spectral range 200-1600 A is adjusted and confirmed

Micro-channel plate gain and phosphor acceleration ranges are verified in the laboratory

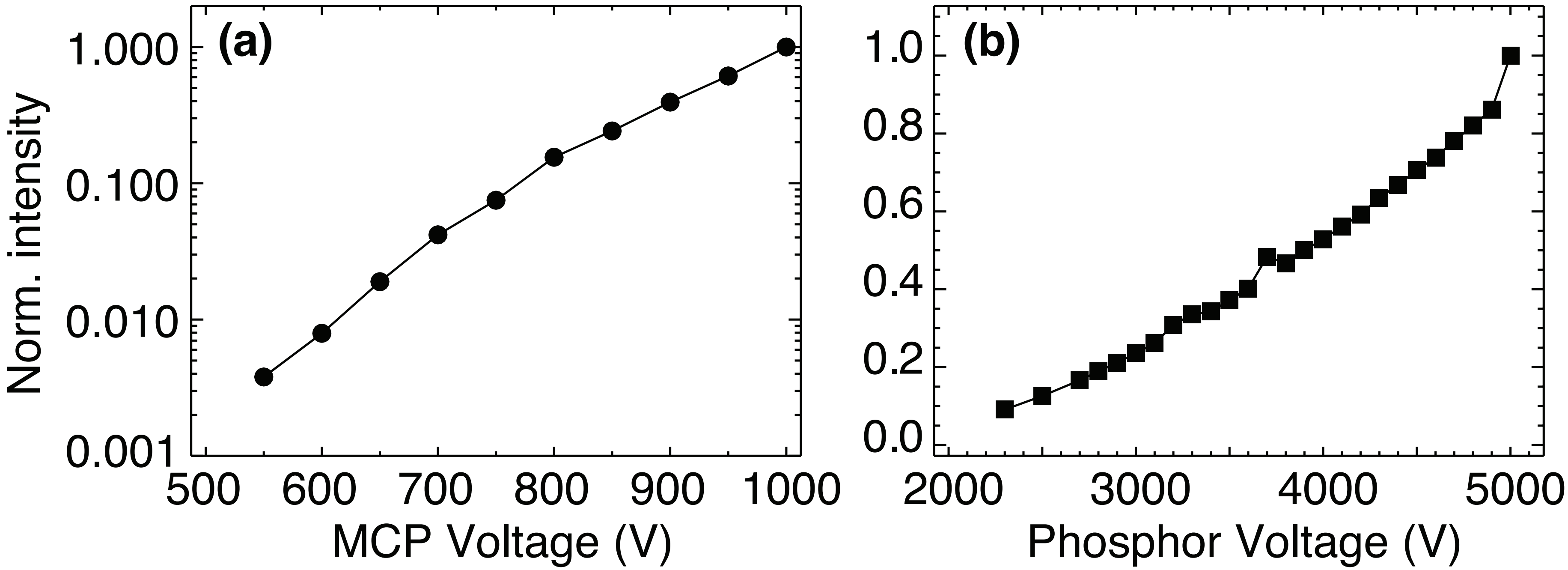

- MCP + CCD tested with Hamamatsu VUV D_2 lamp
- Spectral feature at 1260 A is used
- MCP gain varies over 2.5 orders of magnitude
- Phosphor acceleration can also be varied by factor 10

NBS 1963A Optical resolution target test shows 30 um spatial resolution of optical relay and detector system

- High-frequency NBS 1963A resolution test targets
- Target attached to fiberoptic bundle, lens and CCD
- Resolution about 30 um

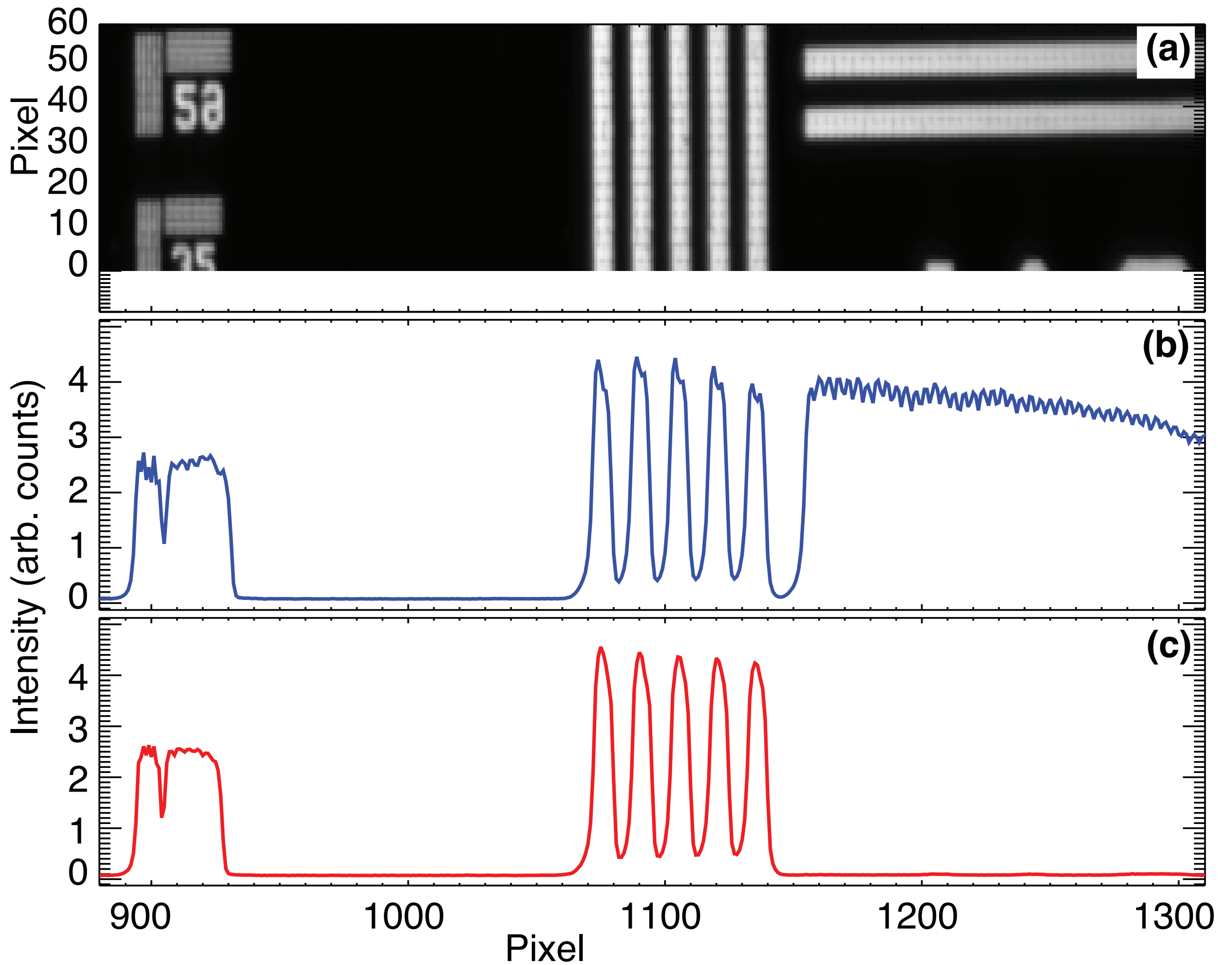

CRETIN code modeling used for T_e sensitivity of D, Li, C spectra

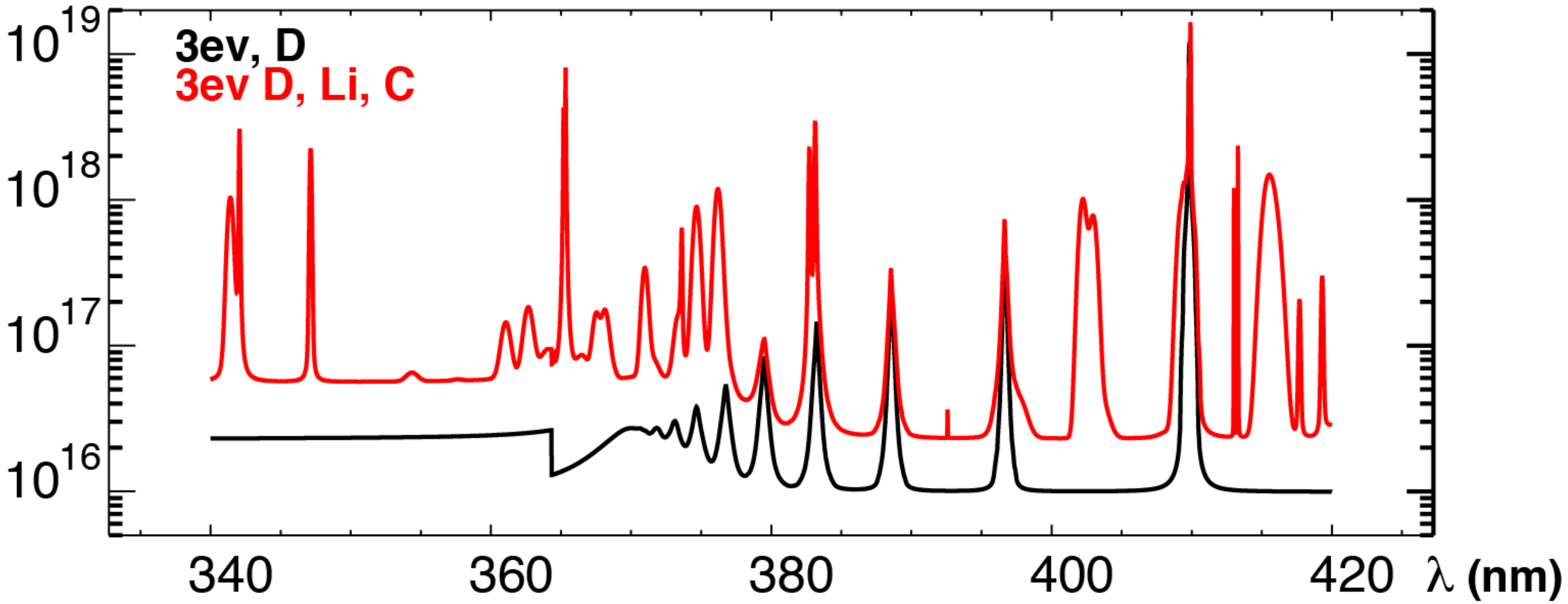

- CRETIN code is a collisional-radiative and radiation transport solver
  - H. Scott, J. Quant. Spectrosc. Radiat. Transf. 71 (2001) 689
  - Calculates whole spectrum including bremsstrahlung, line emission,line profiles, self-absorption, ionization and recombination
  - Includes NLTA population kinetics, radiation transport, neutral diffusion, diagnostic simulators
  - Line profiles code: TOTAL
    - Quasi-static approximation for ions, impact approximation for electrons
    - Electric dipole momentum reduced matrix elements must be calculated elsewhere
- Atomic data either from FAC or from hydrogenic model

Li, C, O spectra simulations with CRETIN demonstrate feasibility of spectroscopic T_e measurements

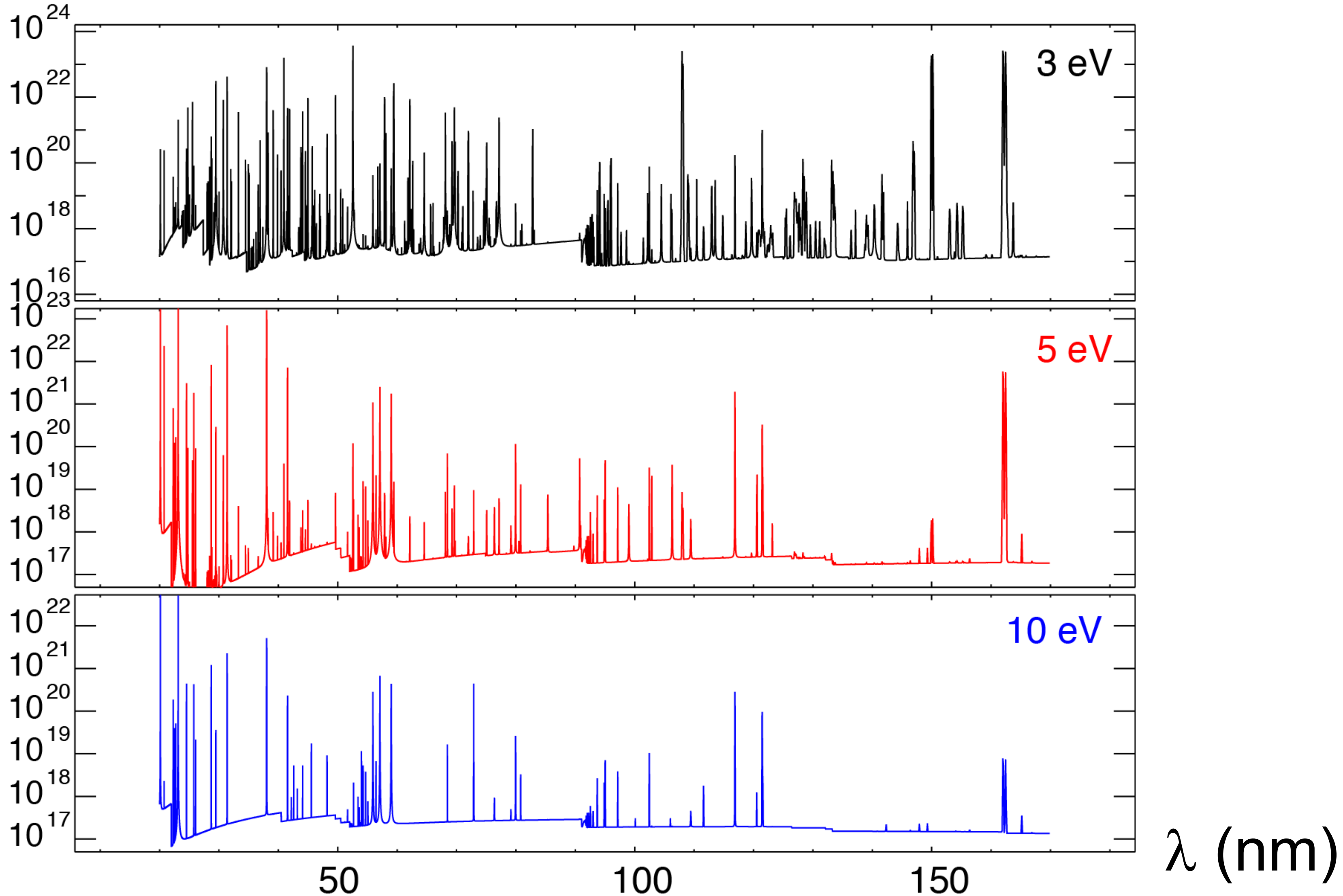

High-*n* Balmer line spectra used in NSTX for divertor recombination rate, T_e and n_e studies

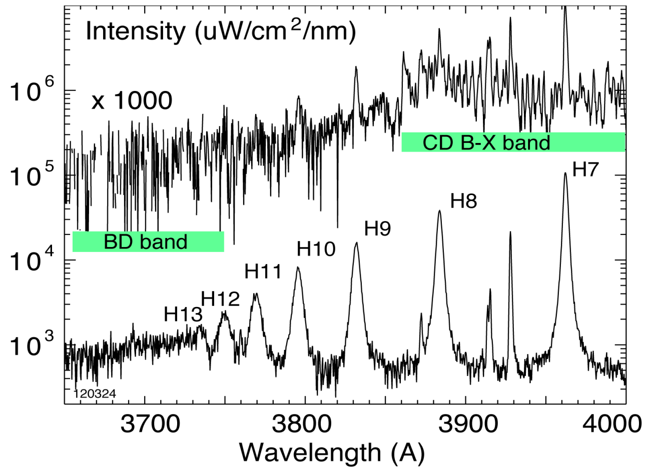

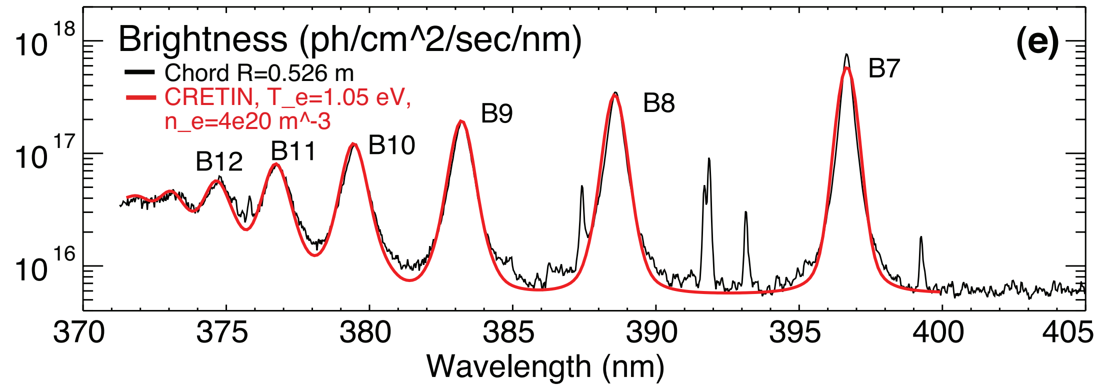

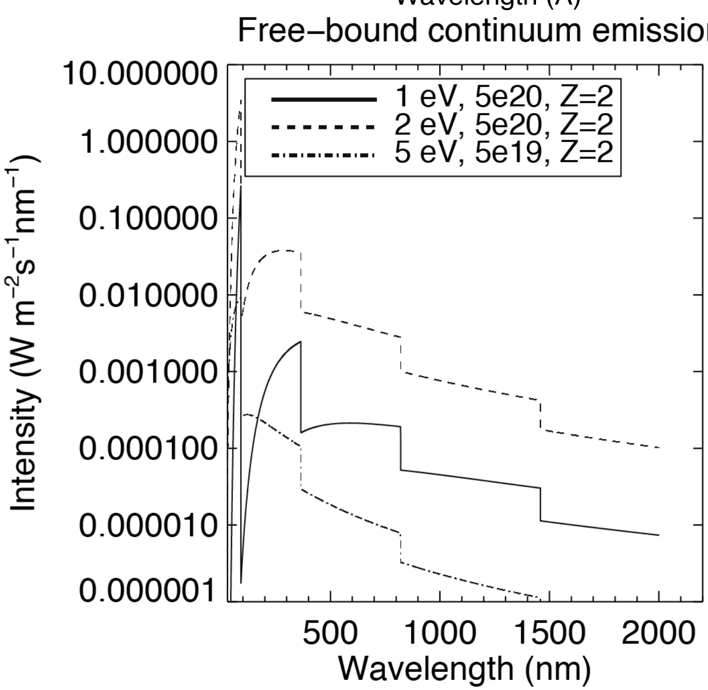

- Balmer series spectra modeled with CRETIN
- T_e=0.8-1.2 eV, n_e=2-7 x 10^{20} m^{-3} inferred from modeling
- Free-bound continuum modeled with CHIANTI

V. A. Soukhanovskii et al., Nucl. Fusion 2011
V. A. Soukhanovskii et al., RSI 2006

Cretin UV spectra simulations demonstrate feasibility of spectroscopic T_e measurements

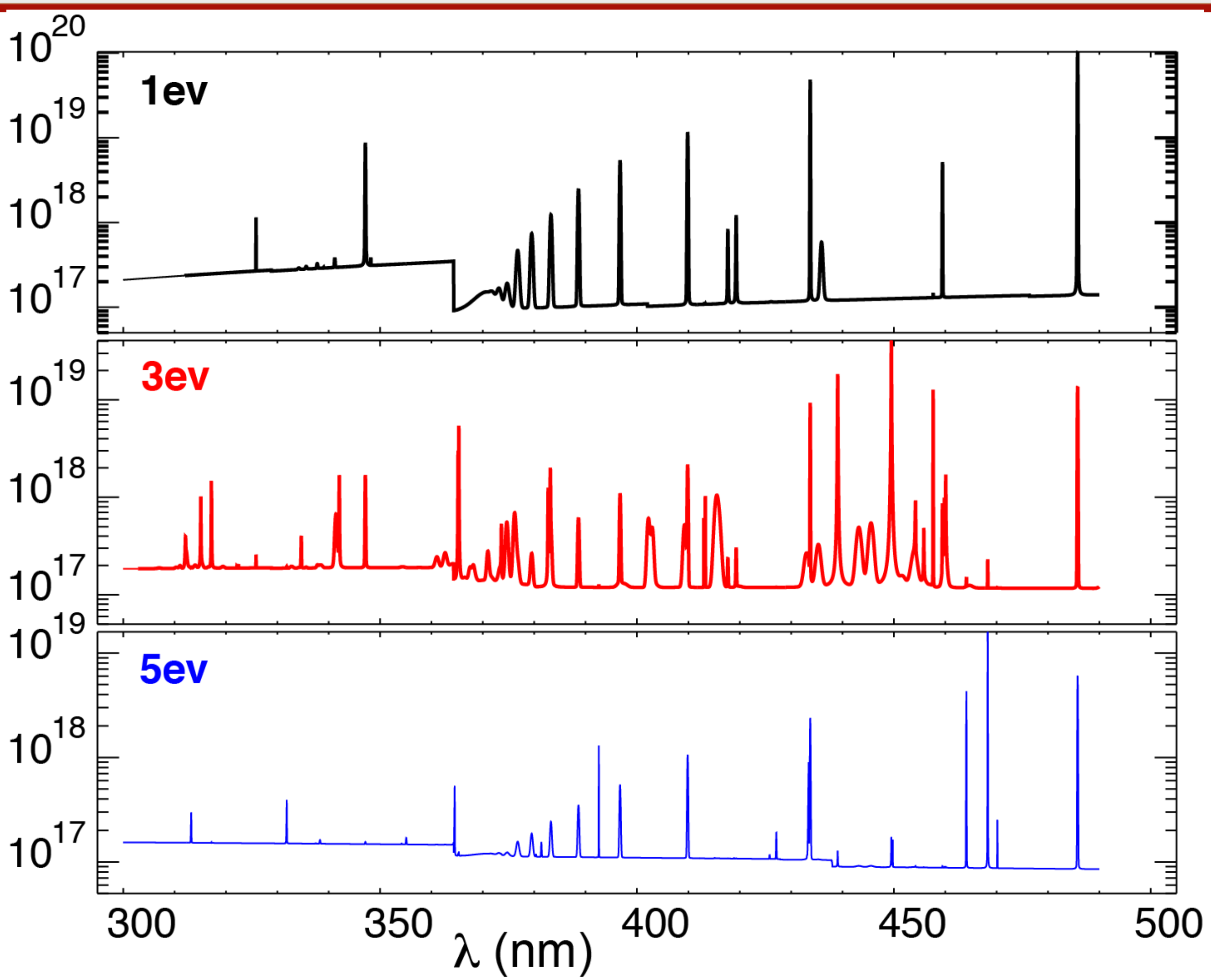

- S

T_e is estimated from Balmer line intensity ratio and from continua intensity ratio at Paschen jump

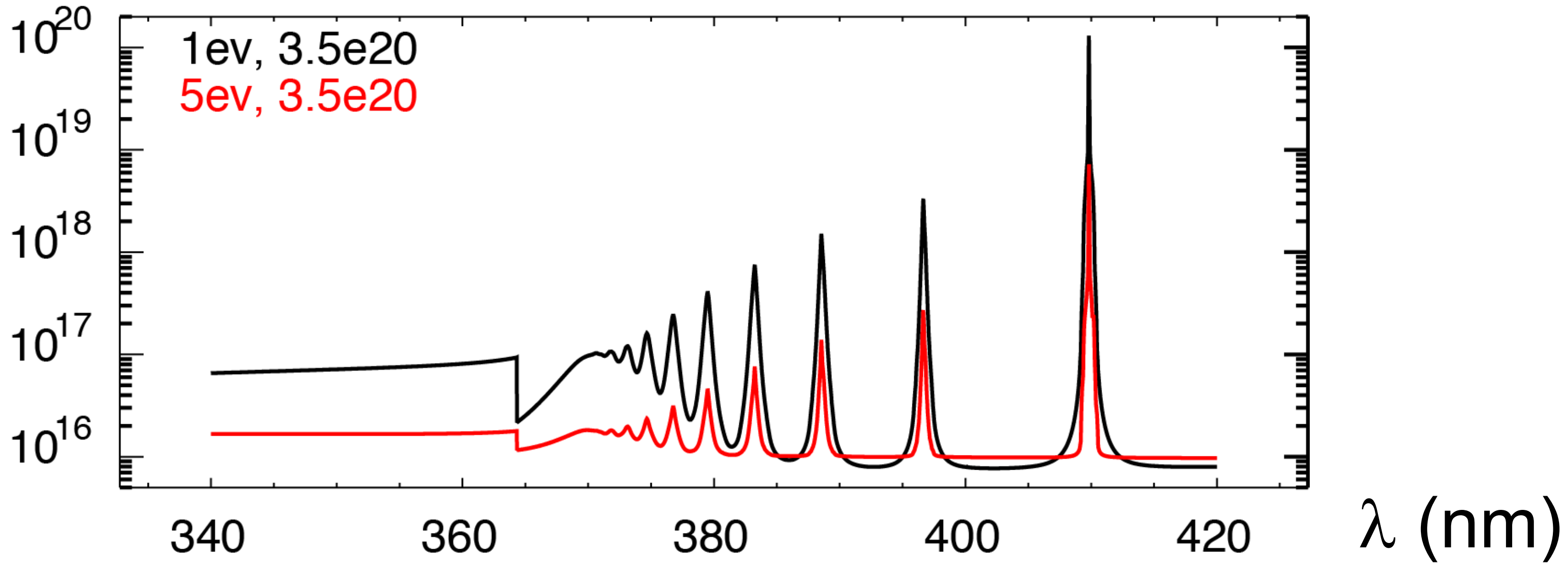

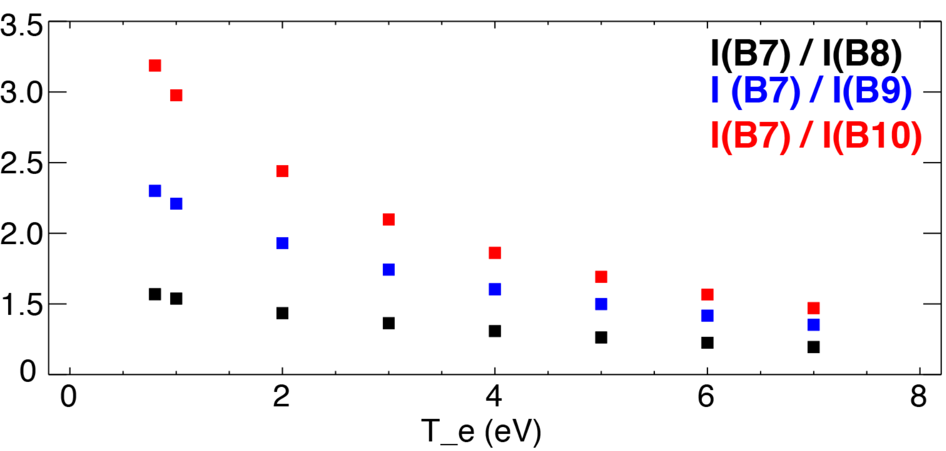

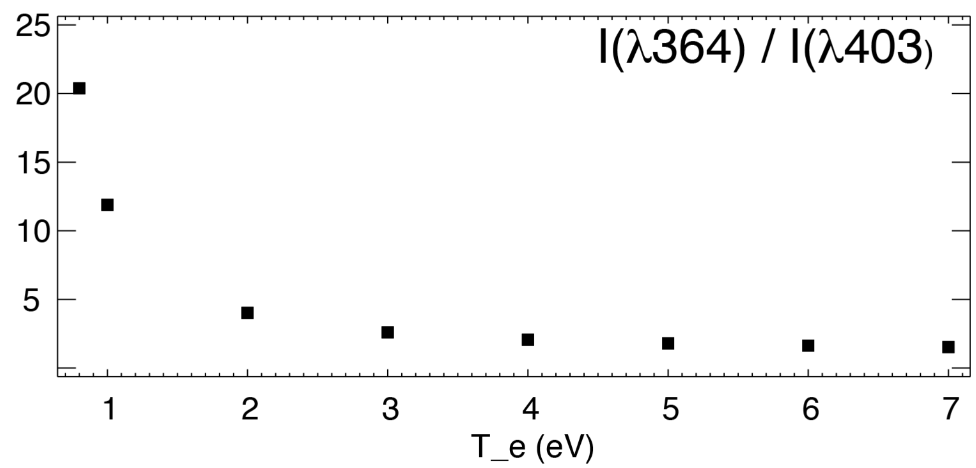

Divertor imaging optics enables quasi-2D divertor emission measurements in UV-VIS-NIR

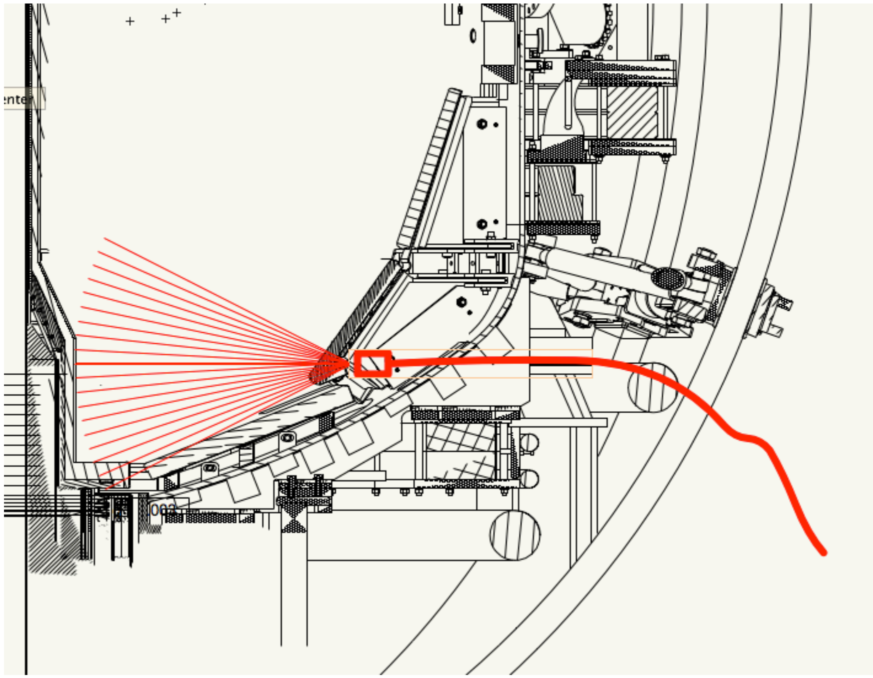

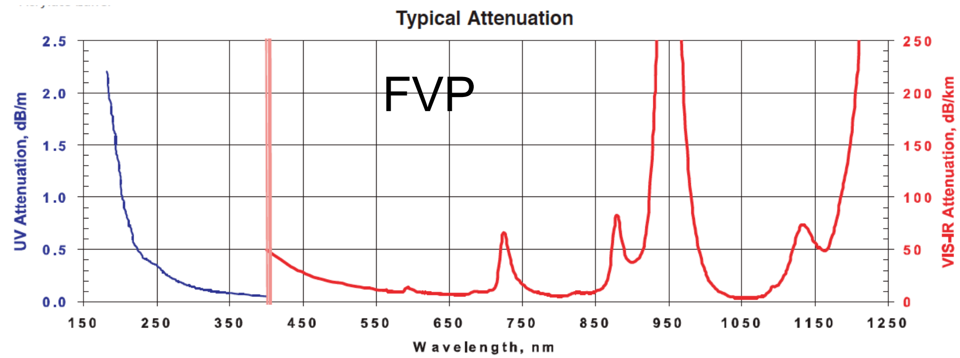

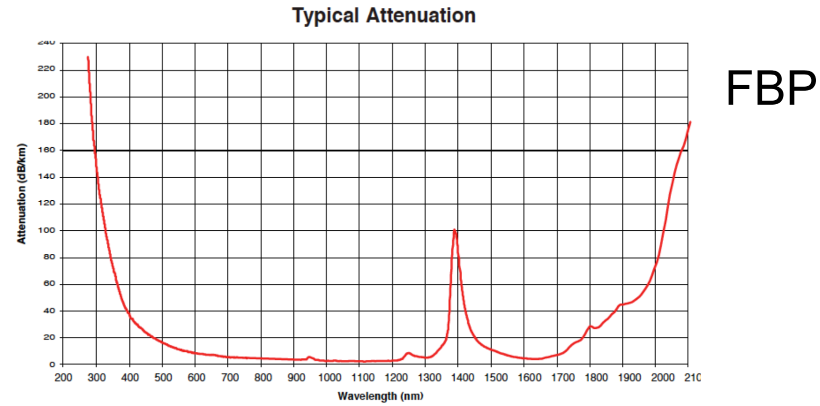

- 26-fiber bundle (Radiation resistant Molex FVP 200 um)
- 10-fiber bundle (Molex FBP 200 um)
- 30 m length
- Kogaku 8 or 12 mm imaging UV lens
- Fiber projection spot size 2-6 mm

Divertor Imaging Balmer Spectrometer (DIBS) enables fast line and continua measurements

- SCT 320 Czerny-Turner-Schmitt spectrograph
  - 600, 1200, 1800 gr/mm UV-VIS 68 mm gratings
- CCD camera PI ProEM 1600x400
- Real-time DAQ via WinSpec32 (pvcam)

Grating l/mm	CWL	Range (nm)	Short wl	Long wl	Dispersion nm/mm	CCD resolution (FWHM)	Bandwidth per pixel
600	399	124	336	461	4.849	0.14	0.078
1200	380 399	59 59	350 369	409 428	2.333 2.321	0.067 0.067	0.037 0.037
1800	399	37	380	417	1.452	0.044	0.023